

Vision to Geometry: 3D Spatial Memory for Sequential Embodied MLLM Reasoning and Exploration

Zhongyi Cai^{1*} Yi Du^{2*} Chen Wang² Yu Kong¹

¹ ACTION Lab, Michigan State University

² SAIR Lab, University at Buffalo

Abstract. Embodied agents are expected to assist humans by actively exploring unknown environments and reasoning about spatial contexts. When deployed in real life, agents often face sequential tasks where each new task follows the completion of the previous one and may include infeasible objectives, such as searching for non-existent objects. However, most existing research focuses on isolated goals, overlooking the core challenge of sequential tasks: the ability to reuse spatial knowledge accumulated from previous explorations to guide subsequent reasoning and exploration. In this work, we investigate this underexplored yet practically significant embodied AI challenge. Specifically, we propose 3DSPMR, a 3D SPatial Memory Reasoning framework that utilizes Field-of-View (FoV) coverage as an explicit geometric prior. By integrating FoV-based constraints, 3DSPMR significantly enhances an agent’s memory, reasoning, and exploration capabilities across sequential tasks. To facilitate research in this area, we further introduce SEER-Bench, a novel Sequential Embodied Exploration and Reasoning Benchmark that spans two foundational tasks: Embodied Question Answering (EQA) and Embodied Multi-modal Navigation (EMN). SEER-Bench uniquely incorporates both feasible and infeasible tasks to provide a rigorous and comprehensive evaluation of agent performance. Extensive experiments verify that 3DSPMR achieves substantial performance gains on both sequential EQA and EMN tasks.

Keywords: Embodied AI · Spatial Reasoning · Spatial Exploration

1 Introduction

In real-world scenarios, embodied agents frequently encounter sequential tasks, where tasks follow one another and may even be infeasible, such as searching for non-existent objects. For feasible tasks, agents should operate efficiently; for infeasible ones, they must detect the impossibility and communicate it clearly. However, mainstream research in Embodied Question Answering (EQA) [7, 12,

* Equal contribution.

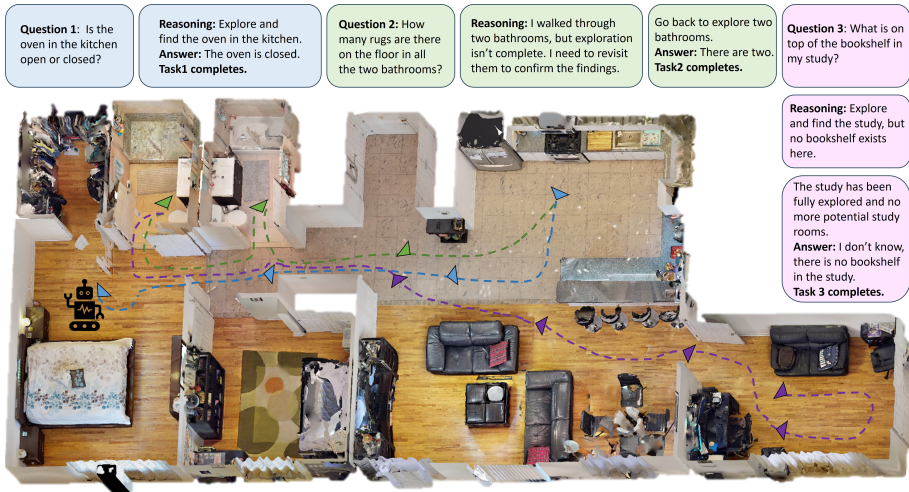


Fig. 1: Illustration of 3DSPMR completing sequential EQA tasks. After navigating to the kitchen and answering the first question, the agent receives a second query. Using its spatial memory, it recognizes two previously passed but insufficiently explored bathrooms, revisits them, and answers the question after sufficient exploration. For the third question, the agent locates the study but cannot find a bookshelf; once the study is fully explored and no alternative candidate rooms remain, 3DSPMR correctly identifies the task as infeasible.

20, 21, 29, 36] and Embodied Multi-modal Navigation (EMN) [3, 24, 42, 44, 46, 49] remains largely confined to a single-task setting [9, 17, 25, 47], where the agent’s memory is reset for each isolated goal. Only a few recent EMN studies [18, 31] have begun to consider sequential settings, yet they still overlook infeasible tasks. To bridge this gap, we investigate this underexplored yet realistic issue of sequential embodied tasks to promote the advancement of embodied agents. The core challenge in this setting lies in enabling agents to effectively reuse spatial information accumulated from prior tasks.

Multi-modal Large Language Models (MLLMs) [6, 16] are powerful general-purpose models that have been applied to complex embodied AI problems, yet they still struggle with spatial understanding and reasoning [5, 39]. Although recent studies [30, 41, 42] have employed memory-based reasoning frameworks to enhance embodied agents in task reasoning and exploration, these approaches face three major challenges when applied to sequential embodied tasks. First, their memory designs either omit essential cues or store excessive redundant details from previously explored areas during earlier tasks, causing agents to struggle with retrieving relevant information for the new task. Second, MLLMs may overconfidently produce premature results or even hallucinations based on partial memory information, due to incomplete exploration in earlier tasks. Finally,

these approaches fail to identify infeasible tasks, leading agents to repeatedly or endlessly explore already well-explored areas.

To address these challenges, we propose 3D SPatial Memory Reasoning (3DSPMR), which introduces explicit geometric cues derived from the Field-of-View (FoV) coverage to simultaneously enhance memory, reasoning, and exploration. As shown in Fig. 2, FoV coverage is defined as the specific set of 2D grid cells that fall within the saved observation’s viewing range. We perform ray casting from the agent’s pose to identify visible cells. Those intersected by rays are marked as “covered” (yellow cells). By modeling FoV coverage, 3DSPMR provides a structured geometric representation of exploration progress.

Specifically, our 3DSPMR framework enhances embodied agents across three critical dimensions. First, for memory construction, we propose a new FoV-based gating mechanism to decide when to save specific observations. As a result, the memory keeps representative data and filters spatial redundancy. Second, for model reasoning, we propose to leverage FoV coverage to verify whether all task-relevant spatial information has been sufficiently collected. This post-inference mechanism enables grounded geometric examination rectifying the MLLM’s predictions to mitigate common failure modes, such as premature task termination and the inability to recognize infeasible requests. Finally, for exploration, we propose utilizing FoV coverage to incentivize exploration of underexplored regions. When triggered, our designed Geometric and Semantic (Geo-Sem) module identifies optimal frontier targets by fusing geometric coverage with task-relevant semantics, resulting in more effective navigation goal selection.

As existing benchmarks mainly annotate single task in each environment and filter out infeasible tasks, we construct the Sequential Embodied Exploration and Reasoning Benchmark (SEER-Bench), which covers EQA and EMN in a sequential setting, to systematically evaluate agent performance. By integrating both feasible and infeasible tasks, SEER-Bench extends the sequential embodied task formulation, offering a rigorous and comprehensive evaluation of an agent’s practical capabilities. Extensive experiments demonstrate that 3DSPMR substantially enhances both reasoning accuracy and exploration efficiency in previously unseen 3D environments.

Our contributions can be summarized as follows:

- We propose a compact and representative spatial memory by employing a FoV-based gating mechanism to filter redundant observations, effectively bridging the 3D scene understanding gap of MLLMs in sequential tasks.
- We develop 3DSPMR, which introduces a grounded geometric examination mechanism and Geo-Sem exploration to enhance reasoning reliability, task feasibility awareness, and exploration efficiency.

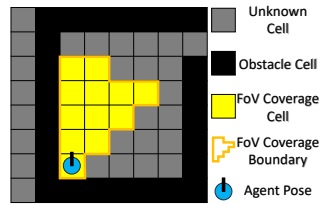


Fig. 2: FoV coverage visualization.

- We propose SEER-Bench, a Sequential Embodied Exploration and Reasoning Benchmark that covers EQA and EMN, including both feasible and infeasible tasks to systematically evaluate agent’s performance.

2 Related Work

MLLMs for Embodied and Spatial Reasoning. Recent Multimodal Large Language Models (MLLMs) such as GPT-4o [16], Qwen2-VL [33], and LLaVA-OneVision [19] have shown remarkable progress in general visual–language reasoning. These models have inspired growing efforts toward embodied and spatial reasoning, where agents interpret 3D environments and perform goal-directed behaviors [11, 23, 26]. However, most existing MLLMs rely on 2D image–text supervision and lack explicit 3D spatial awareness [5, 39]. This limitation constrains their ability to reason about geometry, occlusion, and room layouts, which are crucial for embodied perception and navigation. Moreover, their frame-wise visual processing hinders persistent memory formation, leading to fragmented and inconsistent spatial understanding in long-horizon tasks. As a solution, our proposed 3DSPMR approach leverages a unified spatial memory to distill complex 3D representations into text-form scene graphs, images, and geometric map, providing a more accessible input format for MLLMs.

3D Representations and Memory in Embodied Agents. Structured spatial representations are central to effective reasoning and interaction within 3D environments. Scene-graph-based methods [13–15, 28, 35] encode object relationships and spatial hierarchies, offering interpretable relational abstractions. However, such symbolic graphs are typically sparse and lack the visual richness needed for perceptual grounding. Complementary approaches that store ego-centric visual memories [4, 40, 41] allow retrieval of past observations but often lack geometric or relational awareness. Recent methods [10, 22, 35, 41, 50] have explored constructing 3D semantic maps and global spatial memories, which enhance navigation and question answering yet treat relational, visual, and geometric cues independently. In contrast, 3DSPMR integrates these complementary modalities into a unified 3D spatial memory, combining relational structure, visual appearance, and geometric coverage for coherent spatial reasoning.

Sequential Embodied Tasks. Traditional embodied research such as Embodied Question Answering (EQA) [8, 45] and Scene-Graph Navigation (SG-Nav) [42] evaluate isolated single-task scenarios where each episode is independent. Recent works have explored sequential and multi-task settings [31, 43, 48], but they typically assume all goals or questions are feasible. In realistic environments, some queries are inherently *infeasible*, such as asking for the color of a non-existent object or navigating to an unreachable area. Addressing such cases requires feasibility awareness in addition to spatial reasoning—an ability largely overlooked in prior benchmarks. Recent extensions of EQA, such as OpenEQA [25], GraphEQA [30], and exploration-aware EQA [17], have begun to tackle more diverse and dynamic settings but still do not explicitly incorporate infeasible task reasoning. Our SEER-Bench extends this paradigm by includ-

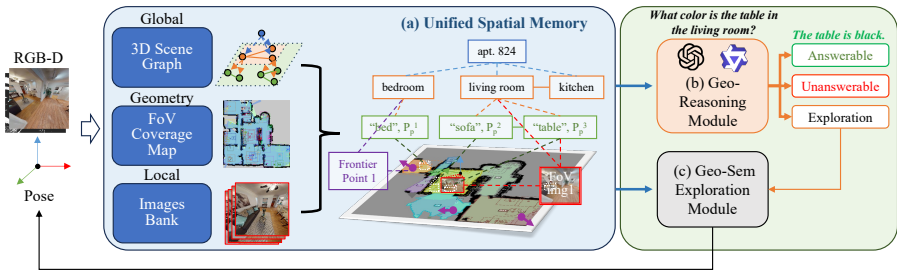


Fig. 3: Overview of the 3DSPMR. (a) Unified Spatial Memory: Raw observations are selectively stored to maintain an informative structured spatial representation. (b) Geo-Reasoning: A grounded inference module that ensures robust decision-making. (c) Geo-Sem Exploration: A strategic module that identifies optimal frontier targets.

ing both feasible and infeasible tasks in sequential EQA and EMN episodes. Therefore, SEER-Bench extends the embodied task formulation, offering a more realistic and comprehensive evaluation for real-world embodied agents.

3 Methodology

In this section, we present the 3DSPMR framework, designed to address the challenges of long-horizon memory retention and task-infeasibility awareness in sequential embodied tasks. As exhibited in Fig. 3, it comprises three synergistic components: a unified spatial memory, a Geo-Reasoning module, and a Geo-Sem Exploration module. The unified spatial memory serves as a structured knowledge base, maintaining a sparse yet informative spatial representation of the environment for efficient multi-task reuse. Building upon this memory, the Geo-Reasoning module performs grounded spatial inference to ensure robust decision-making and task-infeasibility detection. Finally, when Geo-Reasoning determines that further environment discovery is required, the Geometric and Semantic (Geo-Sem) Exploration module identifies optimal frontier targets by integrating visual semantics with geometric incentives.

3.1 Unified Spatial Memory

In sequential embodied tasks, agents must possess the capability to consolidate and reuse historical information gathered across multiple tasks, which necessitates a compact yet representative memory. However, existing memory architectures often fall into two extremes: they either focus exclusively on current-task-specific information [29, 30], or accumulate excessive redundant details [34, 41]. Consequently, when transitioning to new tasks, agents may either suffer from knowledge gaps or become encumbered by irrelevant spatial information.

To address this issue, 3DSPMR constructs a unified spatial memory that continuously aggregates representative information from all observations. These efficient persistent representations enable the agent to either directly facilitate

reasoning, such as answering EQA queries from memory, or guide exploration by leveraging previously collected environmental cues.

As shown in Fig. 3(a), the unified spatial memory comprises three complementary modalities: global relational cues that provide topological context via a 3D scene graph, local visual cues that preserve high-fidelity visual attributes through an ego-centric image bank, and geometric cues derived from a Field-of-View (FoV) coverage map. Notably, we introduce geometric cues to provide a critical anchor for the model to verify task feasibility and completion while facilitating the integration of local and global memory. Furthermore, we introduce FoV-based gating which retains only non-redundant observations, significantly reducing the storage overhead associated with resource-intensive visual data.

Global Relational and Local Visual Cues. Globally, we represent the environment as a hierarchical 3D scene graph G comprising *Apartment*, *Room*, and *Object* levels. Object nodes are maintained via ConceptGraphs [13], while room-level nodes are generated through morphological processing of the 2D occupancy map. Although this graph provides a highly interpretable and structured topological map, it inevitably abstracts away fine-grained visual textures and high-fidelity appearance details. To preserve these critical local observations, we maintain a keyframe image bank I , which serves as a repository for high-resolution ego-centric views. The geometric cues described below determine the timing and selection of image storage to keep I compact and representative.

Geometric Cues. Unlike previous memory designs, we introduce FoV coverage (shown in Fig. 2) as a fundamental geometric cue. Based on this cue, we propose a geometric gating mechanism to maintain a compact image memory. We argue that visual observations should only be stored when they provide significant geometric expansion, effectively providing the system with sufficiently novel spatial information. We define geometric novelty as the proportion of the current view that occupies previously unobserved spatial regions. Specifically, given the current FoV coverage C_{new} (the blue boundary region in Fig. 4) and the accumulated historical coverage $C_{history}$ (the yellow boundary region in Fig. 4), the novelty score τ_{novel} is formulated as:

$$\tau_{novel} = 1 - \frac{|C_{new} \cap C_{history}|}{|C_{new}|}. \quad (1)$$

At step t , if τ_{novel} exceeds a predefined threshold τ_0 , the system commits this image to the image bank I_t and updates the coverage map via $C_t = C_{history} \cup C_{new}$. This union incorporates the newly observed cells (blue cells in Fig. 4). This strategy naturally leads to memory

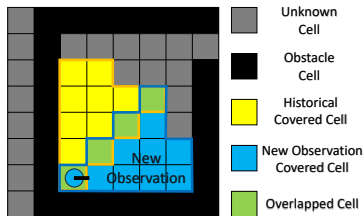


Fig. 4: Visualization of FoV-based Gating. After a 90° rotation, the agent obtains a new observation. Using the historical FoV coverage (yellow cells) and the coverage from the new observation (blue cells), we calculate the overlap (green cells) to decide whether to save this observation.

saturation once the environment is fully explored, effectively filtering redundant views while preserving a representative visual history for sequential tasks.

Beyond filtering, FoV coverage functions as a geometric bridge to establish bidirectional links between 2D keyframe images and 3D graph nodes. Specifically, each saved image in I is indexed to the object nodes within its visibility frustum. Conversely, each object node stores references to all images that encompass it. This cross-modal indexing enables seamless transitions between global and local cues, synthesizing them into a unified memory architecture. Finally, the FoV coverage serves as a quantitative metric for exploration progress. By intersecting the historical FoV coverage $C_{history}$ with the whole area of a specific room S_{room} (e.g., the area of Room 1 enclosed by the blue boundary in Fig. 5), we calculate the coverage rate η to represent the explored proportion of this room:

$$\eta = \frac{|C_{history} \cap S_{room}|}{|S_{room}|}. \quad (2)$$

This metric provides a geometric grounding for the agent to assess each room’s exploration status and serves as a termination criterion for task completion.

Unified Spatial Memory. Together, these cues constitute a unified spatial memory at step t , defined as $\mathcal{M}_t = f_{3DSPMR}(G_t, I_t, C_t)$, where the global 3D scene graph G_t encodes symbolic structure, the local image bank I_t provides perceptual grounding, and the FoV coverage map C_t ensures spatial consistency. At each step t , the agent collects RGB-D observations from its current pose to perceive the local environment. These data are subsequently integrated into the unified spatial memory, as illustrated in Fig. 6. The system first computes the geometric novelty score τ_{novel} (Eq. 1) to decide whether to update C_t and to commit the observation frame to I_t . If the frame is stored, the scene graph is also updated, and bidirectional links are established between the new image and the relevant object nodes. By synchronizing these heterogeneous cues, 3DSPMR bridges the gap in 3D scene understanding for MLLMs, providing a robust foundation for downstream reasoning.

3.2 Geo-Reasoning

Building on the unified spatial memory, we introduce a Geo-Reasoning module designed to utilize multi-modal cues for task execution and infeasibility detection. While MLLMs exhibit remarkable perceptual and reasoning capabilities when processing text and image inputs, they are prone to premature conclusions in partially explored environments and logical loops when facing infeasible

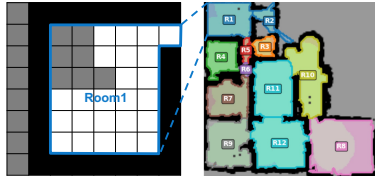


Fig. 5: Room Coverage. The blue boundary defines the area of Room 1, while white cells mark covered regions $C_{history}$. The room coverage ratio is calculated as the fraction of the total room area S_{room} (cells within the boundary) that has been covered by the agent.

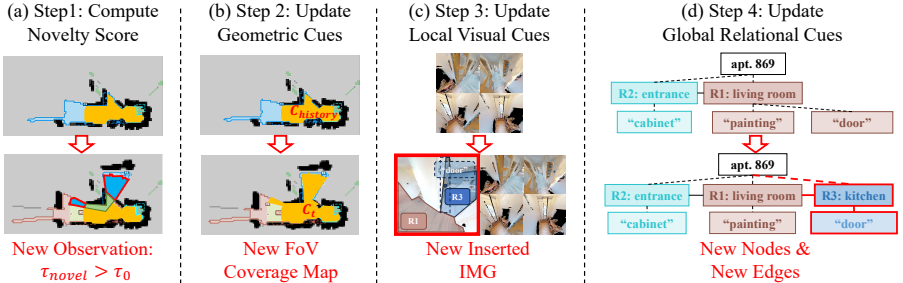


Fig. 6: Unified Spatial Memory Update. The update process comprises four steps. (a) Step 1: compute the novelty score τ_{novel} of new observation. If $\tau_{novel} > \tau_0$, update memory in later steps. (b) Step 2: update geometric cues by merging the historical coverage map with the new image’s FoV coverage. (c) Step 3: update local visual cues by saving this image into the image bank. (d) Step 4: update global relational cues by updating graph and establishing bidirectional links between the graph and the image.

tasks. Unlike prior approaches [17, 29, 30] that rely on model-based confidence heuristics and often suffer from calibration issues, Geo-Reasoning introduces model-agnostic geometric information (*i.e.*, FoV coverage) to provide an unbiased, external verification.

As shown in Fig. 7, Geo-Reasoning operates in two distinct phases: first, Reasoning Modules provide an initial inference; second, a Geometric Examination Mechanism performs post-reasoning validation.

Reasoning Modules. We utilize MLLMs in a training-free, hierarchical manner to interpret the multi-modal cues stored in memory. For the EQA task, the process is executed through four specialized stages: Question Analysis decomposes the query into hierarchical semantic requirements; Global Reasoning prunes the 3D scene graph G to isolate task-relevant sub-graphs; Local Reasoning then retrieves the associated keyframes I indexed by these sub-graphs, further narrowing the visual search space to extract precise perceptual evidence; and Question Answering formulates the final response by synthesizing symbolic and visual evidence. This pipeline effectively distills the complex, multi-modal spatial memory into task-level decisions supported by structured evidence. These initial conclusions are then subject to the Geometric Examination to ensure their geometric grounding.

Geometric Examination Mechanism. The geometric examination leverages the cumulative coverage map C stored in the spatial memory to assess exploration completeness. If the coverage rate η (Eq. 2) of all task-relevant rooms exceeds a predefined threshold, the inference is deemed grounded and accepted. Conversely, if there remains underexplored relevant regions, the mechanism declines the answer and triggers further exploration via Geo-Sem exploration. For accepted cases where an answer is present, the agent commits to it as the final prediction. Otherwise, the mechanism examines the coverage rate of irrelevant rooms to detect existence of any unseen but potentially relevant regions. If no

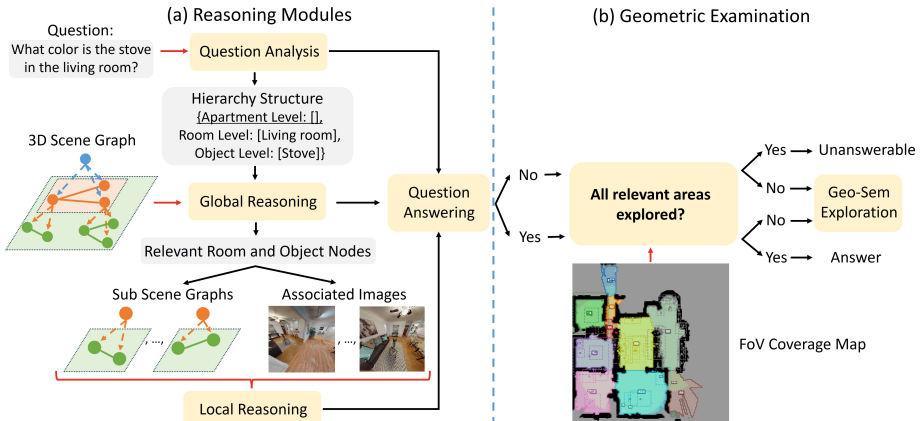


Fig. 7: Illustration of Geo-Reasoning in 3DSPMR for EQA tasks. (a) Phase 1: Reasoning Modules leverage the graph and images in spatial memory to generate an initial inference. (b) Phase 2: Geometric Examination mechanism utilizes FoV coverage to assess task completion. If the relevant spatial regions are fully explored, the system either confirms the inferred answer or flags task infeasibility; otherwise, it triggers Geo-Sem Exploration to determine the next optimal exploration direction.

unexplored areas remain, the query is formally labeled as unanswerable. If unexplored regions persist, the system triggers Geo-Sem exploration to gather additional information. By bridging geometric occupancy with semantic reasoning, this mechanism effectively prevents premature task termination, detects inexecutable tasks, and mitigates redundant revisiting of explored space.

3.3 Geo-Sem Exploration

In scenarios necessitating exploration, the agent is tasked with determining the most informative unexplored region to visit next. Prior works [25, 43] primarily leverage visual semantics from frontier images for navigation; however, such a paradigm ignores critical geometric considerations, which may result in inefficient trajectories, especially when semantic signals alone fail to distinguish between multiple candidates.

The proposed Geo-Sem Exploration module mitigates these deficiencies by integrating geometric cues with visual semantics, enabling the agent to holistically determine the next target region. At each exploration step, the 2D occupancy map identifies a set of frontiers \mathcal{F}_t , defined as the boundary regions between explored (yellow cells) and unexplored unknown space (gray cells). For each frontier node $i \in \mathcal{F}_t$ (the purple point shown in Fig. 8), Geo-Sem utilizes a MLLM r to extract a semantic relevance score $v_t^{\text{sem}}(i)$ with respect to the task query Q and the frontier image in node i , defined as: $v_t^{\text{sem}}(i) = r(i, Q)$. This score quantifies the potential of frontier node i to provide information pertinent to the current task.

Additionally, Geo-Sem utilizes two geometric heuristics to guide exploration. Most notably, frontier node i 's FoV is used to evaluate the potential unseen volume beyond it. Based on this, Geo-Sem calculates the exploration potential score $v_t^{\text{exp}}(i)$ with the following formulation:

$$v_t^{\text{exp}}(i) = \frac{U_t^{\text{FoV}}(i)}{U_{\max}}, \quad (3)$$

where $U_t^{\text{FoV}}(i)$ denotes potential explorable area (red cells in Fig 8), and U_{\max} denotes the largest possible explorable area (the area within the whole red boundary). By incentivizing the agent to prioritize regions with larger unexplored area, our strategy expedites the acquisition of a holistic environmental representation, effectively preventing sub-optimal motion patterns such as repetitive oscillations or excessive detours. To encourage the prioritization of proximal targets, Geo-Sem incorporates the geometric proximity to the frontier as a secondary heuristic. This proximity score, $v_t^{\text{dist}}(i)$, is calculated as: $v_t^{\text{dist}}(i) = 1/(1 + \|p_i - p_t\|/d_{\max})$, where p_t is agent's current pos, p_i is the frontier pos, and d_{\max} serves as a distance normalization constant. This refinement enables the agent to favor closer frontiers, particularly when the aforementioned heuristics yield comparable scores across multiple candidates.

Finally, these factors are integrated into a unified composite score $V_t(i)$ as: $V_t(i) = w_{\text{sem}} v_t^{\text{sem}}(i) + w_{\text{exp}} v_t^{\text{exp}}(i) + w_{\text{dist}} v_t^{\text{dist}}(i)$, with weighting coefficients $(w_{\text{sem}}, w_{\text{exp}}, w_{\text{dist}})$ normalized to sum to 1. The target frontier is selected by maximizing the composite score: $i^* = \arg \max_{i \in \mathcal{F}_t} V_t(i)$.

Once the frontier i^* is chosen, the agent navigates toward its location p_{i^*} using a shortest-path planner within the explored region. Such a multi-faceted integration enables the agent to comprehensively determine the next-best-step, significantly enhancing exploration efficiency through the synergy of semantic intent and geometric viability. In practice, we employ the pathfinder from Habitat-Sim [32] to compute such routes and to advance the agent by small steps at each simulation tick.

4 SEER Benchmark

Overview. Existing benchmarks [9, 25, 29] are mainly designed for single-task cases, which typically provide only one or several tasks per scenario and lack infeasible objectives, rendering them insufficient for a systematic evaluation of sequential embodied reasoning. To bridge this gap, we introduce the Sequential Embodied Exploration and Reasoning Benchmark (SEER-Bench). We define an exploration episode as the comprehensive process of exploring an environment and attempting all assigned tasks. By augmenting each scenario with additional

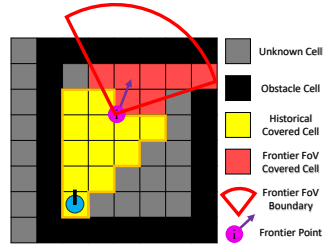


Fig. 8: Frontier Exploration FoV. The red lines delineate the FoV projected ahead of a frontier node. Red cells indicate unknown cells within the FoV, whose area is denoted as U_t^{FoV} in Eq. 3.

annotations, SEER-Bench supports multi-task evaluation within a single episode and assesses an agent’s ability to reuse spatial knowledge and detect infeasible objectives within complex, sequential tasks.

SEER-Bench incorporates two core components: Embodied Question Answering (EQA) and Embodied Multi-modal Navigation (EMN), across 48 scenarios developed using HM3DSem [37] within the Habitat simulator [32]. Each scenario includes 10 tasks, 4 of which are infeasible, providing a realistic foundation for long-horizon sequential embodied reasoning. Comprehensive details regarding annotations and data statistics are provided in the supplementary.

Evaluation Metrics. Suppose the benchmark consists of \mathcal{E} testing episodes, where each episode $e \in \mathcal{E}$ comprises a sequence of N_e tasks. In the EMN part, the agent must navigate to a target goal for each individual task i . We define the success of task i using a binary indicator $S_i \in \{0, 1\}$. For each task i , let l_i denote the shortest path distance from the agent’s initial position at the onset of the task to the goal, and let h_i represent the actual trajectory length traversed by the agent during that specific task.

Standard evaluation metrics, such as Success Rate ($SR = \frac{1}{N} \sum_{i=1}^N S_i$) and Success-weighted Path Length ($SPL = \frac{1}{N} \sum_{i=1}^N S_i \frac{l_i}{\max(h_i, l_i)}$) [1], where $N = \sum_{e \in \mathcal{E}} N_e$ denotes the total number of tasks, effectively measure the correctness and efficiency of isolated single tasks. However, they fail to capture task inter-dependencies or the efficiency of spatial knowledge reuse across a continuous sequence. While one could simply average the SR over tasks within an episode, such an approach often obscures critical failures within the episode.

To address these limitations, we introduce two new metrics that impose strict requirements on long-horizon performance: Sequential Success Rate (SSR) for sequential correctness and Sequential SPL (SSPL) for sequential efficiency.

SSR measures the reliability of an agent across the entire episode. Unlike the average SR, which may award partial credit for completing individual steps, SSR serves as a strict binary metric for the entire episode. We define the success of an episode e using a binary indicator $SR_e \in \{0, 1\}$, which equals 1 if and only if every task within that episode is successfully completed ($S_i = 1$ for all $i \in \{1, \dots, N_e\}$). Thus, SSR reflects the proportion of total episodes \mathcal{E} that achieve full task completion:

$$SSR_{\text{EMN}} = \frac{1}{|\mathcal{E}|} \sum_{e \in \mathcal{E}} \mathbb{I}[SR_e = 1] \times 100\%. \quad (4)$$

SSPL evaluates how efficiently an agent utilizes its total step budget to complete an entire episode. Crucially, this metric serves as a proxy for knowledge reuse: in sequential tasks, maximizing efficiency requires the agent to recall previously explored areas to accelerate subsequent goals, rather than redundantly re-exploring the environment. Let H_e denote the total steps taken by the agent during episode e , and let L_e represent the maximum step budget allocated for that episode. SSPL rewards agents that achieve complete sequential success

($SR_e = 1$) while conserving their step budget:

$$SSPL_{EMN} = \frac{1}{|\mathcal{E}|} \sum_{e \in \mathcal{E}} \left(\mathbb{I}[SR_e = 1] \times \frac{L_e}{\max(H_e, L_e)} \right) \times 100\%. \quad (5)$$

For the Embodied Question Answering (EQA) task, the agent must infer an answer for each question. Consequently, the binary success indicator S_i is replaced by a LLM-based correctness score $\sigma_i \in \{1, \dots, 5\}$ [27] for the inferred answer. In this scale, 1 indicates an incorrect response, 5 signifies a fully correct response, and intermediate values represent varying degrees of semantic similarity to the ground truth. We adopt the correctness and efficiency metrics defined in [27] as SR and SPL. To adapt the SSR for EQA, we consider a task successful if its score σ_i is larger than 3. Based on this threshold, we generalize Eq. 4 to account for the nuanced scores:

$$SSR_{EQA} = \frac{1}{|\mathcal{E}|} \sum_{e \in \mathcal{E}} \frac{\max(0, \sum_{i=1}^{N_e} (\sigma_i - 3))}{2 \times N_e} \times 100\%. \quad (6)$$

Similarly, the SSPL for the EQA part is adapted from Eq. 5 used for EMN. We provide details on the setting of H_e and L_e in the supplementary.

5 Experiment

5.1 Experiment Settings

Setup. Using SEER-Bench, we evaluated an agent’s capacity for multi-step reasoning and active exploration across both the EQA and EMN tracks. For our experimental setup, we constructed a testing dataset by sampling from the 10 annotated tasks in each of the 48 scenarios. Specifically, for each scenario, we randomly selected three feasible and two infeasible tasks. These five tasks were then shuffled to create a sequential task chain, resulting in a total of 240 tasks in each track. The EQA track maintains a wide diversity of question types which include functional, counting, and spatial relationships, and incorporates both answerable and unanswerable queries to test the agent’s discernment. The EMN track features diverse goal modalities, requiring the agent to navigate based on Object, Language, or Image targets. Furthermore, we extended our evaluation by adapting one existing active EQA dataset, HM-EQA [29]. We identified scenarios containing multiple single tasks previously tested in isolation and merged them into sequential episodes. Following the SEER-Bench annotation protocol, we introduced unanswerable questions and randomly selected two infeasible tasks to append to these merged sequences. Through this process, we curated an additional 48 scenarios comprising 240 tasks for testing. Detailed implementations and hyper-parameter configurations are provided in the supplementary.

Baselines. We benchmarked our approach against several representative methods across the EQA and EMN tracks to validate the efficacy of 3DSPMR. Specifically, we compared our method with two representative memory-enhanced active exploration baselines: Explore-Mem [29] and 3D-Mem [41], both utilizing

Table 1: SEER-Bench EQA Results.

Method	SSR \uparrow	SSPL \uparrow	SR \uparrow	SPL \uparrow
<i>Blind LLMs</i>				
Qwen3	0.8	\	24.5	\
GPT-5	0.4	\	24.4	\
<i>Open-Sourced Qwen2.5VL Exploration</i>				
Explore-Mem	0	0	18.2	5.7
3D-Mem	1.8	0.9	32.0	20.9
3DSPMR w/o Geo	2.7	2.0	31.7	28.3
3DSPMR (Ours)	6.7	5.4	42.9	33.9
<i>Close-Sourced GPT-5 Exploration</i>				
3D-Mem	4.5	2.0	35.9	32.7
3DSPMR w/o Geo	6.4	3.3	35.5	28.2
3DSPMR (Ours)	28.2	21.0	55.9	42.5

Table 2: SEER-Bench EMN Results.

Method	SSR \uparrow	SSPL \uparrow	SR \uparrow	SPL \uparrow
<i>GOAT-Bench Baselines</i>				
Modular GOAT	10.4	5.2	24.6	17.1
SenseAct-NN	0.0	0.0	10.4	7.8
<i>Open-Sourced Qwen2.5VL Exploration</i>				
Explore-Mem	2.1	1.5	22.1	10.4
3D-Mem	12.5	4.6	31.7	17.7
3DSPMR w/o Geo	20.8	6.5	50.8	44.3
3DSPMR (Ours)	35.4	15.9	59.2	49.5
<i>Close-Sourced GPT-5 Exploration</i>				
3D-Mem	18.8	6.7	41.7	29.3
3DSPMR w/o Geo	22.9	16.2	54.6	47.5
3DSPMR (Ours)	39.6	27.1	65.0	54.2

Qwen2.5-VL-72B [2] as the default backbone across both tracks. To ensure a rigorous comparison with the state-of-the-art 3D-Mem, we further conducted evaluations using GPT-5 [27] as the backbone for both 3D-Mem and our method. To isolate the influence of geometric information within our proposed 3DSPMR, we conducted an ablation study by removing the FoV-based geometric examination mechanism during reasoning and the geometric heuristics during exploration.

For the EQA track, we additionally incorporated Blind LLMs, specifically Qwen3-14B [38] and GPT-5 [27], to serve as a lower bound by attempting to answer questions without active navigation. In the EMN track, we further evaluated two distinct architectures: Modular GOAT [4], a zero-shot modular baseline lacking persistent memory, and SenseAct-NN [18], a monolithic RL baseline.

5.2 Discussion and Analysis

In this subsection, we present a detailed discussion and analysis of the experimental results. Quantitative performance on SEER-Bench is summarized in Table 1 for the EQA track and Table 2 for the EMN track. In addition, the comparative results on the adapted HM-EQA dataset are presented in Table 3. **Superiority in Sequential Reasoning.** As shown in these tables, 3DSPMR consistently outperforms all baseline methods across every evaluation metric and benchmark. Standard baselines struggle significantly with the more rigorous SSR and SSPL metrics. Specifically, Explore-Mem maintains memory for the current task, failing to reuse information for subsequent queries. While 3D-Mem utilizes an object-clustering memory, it is still inferior to 3DSPMR in both task-

Table 3: Experiments on adapted HM-EQA dataset.

Method	SSR \uparrow	SSPL \uparrow	SR \uparrow	SPL \uparrow
<i>Blind LLMs</i>				
Qwen3	0	\	20.7	\
GPT-5	0.8	\	19.9	\
<i>Open-Sourced Qwen2.5VL Exploration</i>				
Explore-Mem	0.8	0.2	22.0	9.2
3D-Mem	3.5	2.1	29.2	18.0
3DSPMR w/o Geo	2.4	1.5	35.9	25.6
3DSPMR (Ours)	10.8	9.7	46.2	38.8

level (SR, SPL) and episode-level (SSR, SSPL) metrics because it lacks explicit infeasibility detection and fails in preventing premature completion.

In contrast, the superior SR and SPL scores demonstrate that 3DSPMR is more resilient and efficient in challenging environments where infeasible queries are present. Furthermore, the significant gains in SSR and SSPL underscore the 3DSPMR’s robust capability for spatial knowledge reuse. By leveraging a unified spatial memory alongside FoV-guided reasoning and exploration, our agent recalls information from previous steps and reduces redundant explorations. This enables the agent to more effectively address the fundamental challenges of long-horizon, sequential embodied tasks.

Memory Efficiency. To validate the compactness of the unified spatial memory in 3DSPMR, we further compared the memory efficiency with current SOTA 3D-Mem. Specifically, we averaged the number of saved images in each episode for experiments on SEER-Bench. As shown in Fig. 9, 3DSPMR reduces image memory usage by 40.8% on EQA and 30.4% on EMN. 3DSPMR stores substantially fewer images than 3D-Mem which retains observations based on object-clustering. The reduction arises from our FoV-driven gating mechanism, which filters redundant observations while retaining essential visual information. This is an important capability for avoiding memory saturation in long-horizon sequential tasks. Therefore, beyond reasoning improvements, our 3DSPMR features a highly efficient and compact memory system.

Ablation study. We conducted an ablation study on geometric cues by removing FoV-based mechanisms in reasoning and exploration (*3DSPMR w/o Geo*). As shown in the tables, across all three experiments, removing the FoV-based mechanisms leads to a sharp decline in both accuracy and efficiency (*e.g.*, SSPL drops by $\sim 11\%$ in EMN with GPT5). Without the geometric awareness, MLLMs exhibit two failure modes: (1) premature termination, where the agent hallucinates an answer/success before fully exploring; and (2) endless exploration, where the agent moving back and forth in explored area. 3DSPMR’s geometric awareness effectively curbs both behaviors and boosts both accuracy and efficiency. The ablation study highlights the necessity of our explicit geometric modeling. More experiments are provided in supplementary.

6 Conclusion

We propose 3DSPMR, an approach that augments MLLMs with a unified 3D spatial memory integrating explicit geometric FoV coverage, to address challenges in sequential embodied tasks. This geometric grounding effectively enhances spatial reasoning and optimizes exploration efficiency. Furthermore, we

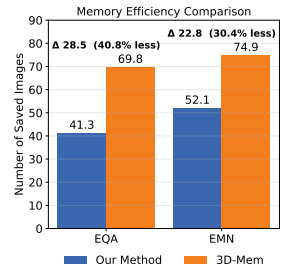


Fig. 9: Memory Efficiency Comparison. On both tracks of SEER-Bench, 3DSPMR saves significantly fewer images than 3D-Mem in the memory.

introduce SEER-Bench, a rigorous framework to comprehensively evaluate embodied agents on sequential, feasibility-aware tasks. Experiments demonstrate that 3DSPMR achieves state-of-the-art performance in sequential embodied tasks, delivering superior correctness and efficiency. Future work will focus on extending this approach to dynamic environments and facilitating sim-to-real transfer.

References

1. Anderson, P., Chang, A., Chaplot, D.S., Dosovitskiy, A., Gupta, S., Koltun, V., Kosecka, J., Malik, J., Mottaghi, R., Savva, M., et al.: On evaluation of embodied navigation agents. arXiv preprint arXiv:1807.06757 (2018)
2. Bai, S., Chen, K., Liu, X., Wang, J., Ge, W., Song, S., Dang, K., Wang, P., Wang, S., Tang, J., et al.: Qwen2. 5-vl technical report. arXiv preprint arXiv:2502.13923 (2025)
3. Batra, D., Gokaslan, A., Kembhavi, A., Maksymets, O., Mottaghi, R., Savva, M., Toshev, A., Wijmans, E.: Objectnav revisited: On evaluation of embodied agents navigating to objects. arXiv preprint arXiv:2006.13171 (2020)
4. Chang, M., Gervet, T., Khanna, M., Yenamandra, S., Shah, D., Min, S.Y., Shah, K., Paxton, C., Gupta, S., Batra, D., et al.: Goat: Go to any thing. arXiv preprint arXiv:2311.06430 (2023)
5. Chen, S., Zhu, T., Zhou, R., Zhang, J., Gao, S., Niebles, J.C., Geva, M., He, J., Wu, J., Li, M.: Why is spatial reasoning hard for vlms? an attention mechanism perspective on focus areas. arXiv preprint arXiv:2503.01773 (2025)
6. Comanici, G., Bieber, E., Schaekermann, M., Pasupat, I., Sachdeva, N., Dhillon, I., Blistein, M., Ram, O., Zhang, D., Rosen, E., et al.: Gemini 2.5: Pushing the frontier with advanced reasoning, multimodality, long context, and next generation agentic capabilities. arXiv preprint arXiv:2507.06261 (2025)
7. Dang, R., Yuan, Y., Zhang, W., Xin, Y., Zhang, B., Li, L., Wang, L., Zeng, Q., Li, X., Bing, L.: Ecbench: Can multi-modal foundation models understand the egocentric world? a holistic embodied cognition benchmark. In: Proceedings of the Computer Vision and Pattern Recognition Conference. pp. 24593–24602 (2025)
8. Das, A., Datta, S., Gkioxari, G., Lee, S., Parikh, D., Batra, D.: Embodied question answering. In: Proceedings of the IEEE conference on computer vision and pattern recognition. pp. 1–10 (2018)
9. Deitke, M., Han, W., Herrasti, A., Kembhavi, A., Kolve, E., Mottaghi, R., Salvador, J., Schwenk, D., VanderBilt, E., Wallingford, M., et al.: Robothor: An open simulation-to-real embodied ai platform. In: Proceedings of the IEEE/CVF conference on computer vision and pattern recognition. pp. 3164–3174 (2020)
10. Du, Y., Fu, T., Chen, Z., Li, B., Su, S., Zhao, Z., Wang, C.: Vl-nav: Real-time vision-language navigation with spatial reasoning. arXiv preprint arXiv:2502.00931 (2025)
11. Goetting, D., Singh, H.G., Loquercio, A.: End-to-end navigation with vision-language models: Transforming spatial reasoning into question-answering. In: Proceedings of the 41st International Conference on Machine Learning (2025), <https://proceedings.mlr.press/v288/goetting25a.html>, pMLR
12. Gordon, D., Kembhavi, A., Rastegari, M., Redmon, J., Fox, D., Farhadi, A.: Iqa: Visual question answering in interactive environments. In: Proceedings of the IEEE/CVF Conference on Computer Vision and Pattern Recognition (CVPR) (2018), https://openaccess.thecvf.com/content_cvpr_2018/papers/Gordon_IQA_Visual_Question_CVPR_2018_paper.pdf
13. Gu, Q., Kuwajerwala, A., Morin, S., Jatavallabhula, K.M., Sen, B., Agarwal, A., Rivera, C., Paul, W., Ellis, K., Chellappa, R., et al.: Conceptgraphs: Open-vocabulary 3d scene graphs for perception and planning. In: 2024 IEEE International Conference on Robotics and Automation (ICRA). pp. 5021–5028. IEEE (2024)

14. Hughes, N., Chang, Y., Carlone, L.: Hydra: A real-time spatial perception system for 3d scene graph construction and optimization. arXiv preprint arXiv:2201.13360 (2022)
15. Hughes, N., Chang, Y., Hu, S., Talak, R., Abdulhai, R., Strader, J., Carlone, L.: Foundations of spatial perception for robotics: Hierarchical representations and real-time systems. *The International Journal of Robotics Research* **43**(10), 1457–1505 (2024)
16. Hurst, A., et al.: Gpt-4o system card. arXiv preprint arXiv:2410.21276 (2024), <https://arxiv.org/abs/2410.21276>
17. Jiang, K., Liu, Y., Chen, W., Luo, J., Chen, Z., Pan, L., Li, G., Lin, L.: Beyond the destination: A novel benchmark for exploration-aware embodied question answering. arXiv preprint arXiv:2503.11117 (2025), <https://arxiv.org/abs/2503.11117>
18. Khanna, M., Ramrakhya, R., Chhablani, G., Yenamandra, S., Gervet, T., Chang, M., Kira, Z., Chaplot, D.S., Batra, D., Mottaghi, R.: Goat-bench: A benchmark for multi-modal lifelong navigation. In: *Proceedings of the IEEE/CVF Conference on Computer Vision and Pattern Recognition*. pp. 16373–16383 (2024)
19. Li, B., Zhang, Y., Guo, D., Zhang, R., Li, F., Zhang, H., Zhang, K., Li, Y., Liu, Z., Li, C.: Llava-onevision: Easy visual task transfer. arXiv preprint arXiv:2408.03326 (2024), <https://arxiv.org/abs/2408.03326>
20. Li, Y., Chen, Y., Dao, A., Li, L., Cai, Z., Tan, Z., Chen, T., Kong, Y.: Industryeqa: Pushing the frontiers of embodied question answering in industrial scenarios. arXiv preprint arXiv:2505.20640 (2025)
21. Linghu, X., Huang, J., Niu, X., Ma, X.S., Jia, B., Huang, S.: Multi-modal situated reasoning in 3d scenes. *Advances in Neural Information Processing Systems* **37**, 140903–140936 (2024)
22. Liu, R., et al.: Volumetric environment representation for vision-language navigation. In: *Proceedings of the IEEE/CVF Conference on Computer Vision and Pattern Recognition (CVPR)* (2024), https://openaccess.thecvf.com/content/CVPR2024/html/Liu_Volumetric_Environment_Representation_for_Vision-Language_Navigation_CVPR_2024_paper.html
23. Liu, S., Wu, Y., Li, L., et al.: Llava-plus: Learning to use tools for creating multimodal agents. In: *ECCV* (2024), https://www.ecva.net/papers/eccv_2024/papers_ECCV/papers/06341.pdf
24. Long, Y., Cai, W., Wang, H., Zhan, G., Dong, H.: Instructnav: Zero-shot system for generic instruction navigation in unexplored environment. arXiv preprint arXiv:2406.04882 (2024)
25. Majumdar, A., Yadav, K., Hoffman, J., Batra, D., Parikh, D., Das, A., Jain, A., Goswami, V., et al.: Openeqa: Embodied question answering in the era of foundation models. arXiv preprint arXiv:2403.12086 (2024), <https://arxiv.org/abs/2403.12086>
26. Mu, Y., Zhang, Q., Hu, M., Wang, W., Ding, M., Jin, J., Wang, B., Dai, J., Qiao, Y., Luo, P.: Embodiedgpt: Vision-language pre-training via embodied chain of thought. arXiv preprint arXiv:2305.15021 (2023), <https://arxiv.org/abs/2305.15021>
27. OpenAI: Gpt-5 technical overview. <https://openai.com> (2025)
28. Rana, K., Haviland, J., Garg, S., Abou-Chakra, J., Reid, I., Suenderhauf, N.: Sayplan: Grounding large language models using 3d scene graphs for scalable robot task planning. arXiv preprint arXiv:2307.06135 (2023)
29. Ren, A.Z., Clark, J., Dixit, A., Itkina, M., Majumdar, A., Sadigh, D.: Explore until confident: Efficient exploration for embodied question answering. arXiv preprint arXiv:2403.15941 (2024)

30. Saxena, S., Buchanan, B., Paxton, C., Chen, B., Vaskevicius, N., Palmieri, L., Francis, J., Kroemer, O.: Grapheqa: Using 3d semantic scene graphs for real-time embodied question answering. arXiv preprint arXiv:2412.14480 (2024), <https://arxiv.org/abs/2412.14480>
31. Song, X., Chen, W., Liu, Y., Chan, V., Li, G., Lin, L.: Towards long-horizon vision-language navigation: Platform, benchmark and method. In: Proceedings of the IEEE/CVF Conference on Computer Vision and Pattern Recognition (CVPR) (2025), https://openaccess.thecvf.com/content/CVPR2025/papers/Song_Towards_Long-Horizon_Vision-Language_Navigation_Platform_Benchmark_and_Method_CVPR_2025_paper.pdf
32. Szot, A., Clegg, A., Undersander, E., Wijmans, E., Zhao, Y., Turner, J., Maestre, N., Mukadam, M., Chaplot, D.S., Maksymets, O., et al.: Habitat 2.0: Training home assistants to rearrange their habitat. *Advances in neural information processing systems* **34**, 251–266 (2021)
33. Wang, P., et al.: Qwen2-vl: Enhancing vision-language model’s visual perception and generative capabilities. arXiv preprint arXiv:2409.12191 (2024), <https://arxiv.org/abs/2409.12191>
34. Wang, S., Wang, Y., Li, W., Cai, X., Wang, Y., Chen, M., Wang, K., Su, Z., Li, D., Fan, Z.: Aux-think: Exploring reasoning strategies for data-efficient vision-language navigation. arXiv preprint arXiv:2505.11886 (2025)
35. Werby, A., Huang, C., Büchner, M., Valada, A., Burgard, W.: Hierarchical open-vocabulary 3d scene graphs for language-grounded robot navigation. In: *Robotics: Science and Systems (RSS)* (2024), <https://www.roboticsproceedings.org/rss20/p077.pdf>
36. Wijmans, E., Datta, S., Maksymets, O., Das, A., Gkioxari, G., Lee, S., Essa, I., Parikh, D., Batra, D.: Embodied question answering in photorealistic environments with point cloud perception. In: *Proceedings of the IEEE/CVF Conference on Computer Vision and Pattern Recognition*. pp. 6659–6668 (2019)
37. Yadav, K., Ramrakhya, R., Ramakrishnan, S.K., Gervet, T., Turner, J., Gokaslan, A., Maestre, N., Chang, A.X., Batra, D., Savva, M., et al.: Habitat-matterport 3d semantics dataset. In: *Proceedings of the IEEE/CVF Conference on Computer Vision and Pattern Recognition*. pp. 4927–4936 (2023)
38. Yang, A., Li, A., Yang, B., Zhang, B., Hui, B., Zheng, B., Yu, B., Gao, C., Huang, C., Lv, C., et al.: Qwen3 technical report. arXiv preprint arXiv:2505.09388 (2025)
39. Yang, J., Yang, S., Gupta, A.W., Han, R., Fei-Fei, L., Xie, S.: Thinking in space: How multimodal large language models see, remember, and recall spaces. In: *Proceedings of the Computer Vision and Pattern Recognition Conference*. pp. 10632–10643 (2025)
40. Yang, Y., Zhou, T., Li, K., Tao, D., Li, L., Shen, L., He, X., Jiang, J., Shi, Y.: Embodied multi-modal agent trained by an llm from a parallel textworld. In: *Proceedings of the IEEE/CVF Conference on Computer Vision and Pattern Recognition (CVPR)* (2024), https://openaccess.thecvf.com/content/CVPR2024/papers/Yang_Embodied_Multi-Modal_Agent_trained_by_an_LLM_from_a_Parallel_CVPR_2024_paper.pdf
41. Yang, Y., Yang, H., Zhou, J., Chen, P., Zhang, H., Du, Y., Gan, C.: 3d-mem: 3d scene memory for embodied exploration and reasoning. In: *Proceedings of the Computer Vision and Pattern Recognition Conference*. pp. 17294–17303 (2025)
42. Yin, H., Xu, X., Wu, Z., Zhou, J., Lu, J.: Sg-nav: Online 3d scene graph prompting for llm-based zero-shot object navigation. *Advances in neural information processing systems* **37**, 5285–5307 (2024)

43. Yin, H., Xu, X., Zhao, L., Wang, Z., Zhou, J., Lu, J.: Unigoal: Towards universal zero-shot goal-oriented navigation. In: Proceedings of the IEEE/CVF Conference on Computer Vision and Pattern Recognition (CVPR) (2025), https://openaccess.thecvf.com/content/CVPR2025/papers/Yin_UniGoal_Towards_Universal_Zero-shot_Goal-oriented_Navigation_CVPR_2025_paper.pdf
44. Yokoyama, N., Ramrakhya, R., Das, A., Batra, D., Ha, S.: Hm3d-ovon: A dataset and benchmark for open-vocabulary object goal navigation. In: 2024 IEEE/RSJ International Conference on Intelligent Robots and Systems (IROS). pp. 5543–5550. IEEE (2024)
45. Yu, L., Chen, X., Gkioxari, G., Bansal, M., Berg, T.L., Batra, D.: Multi-target embodied question answering. In: Proceedings of the IEEE/CVF Conference on Computer Vision and Pattern Recognition. pp. 6309–6318 (2019)
46. Zhang, J., Dai, L., Meng, F., Fan, Q., Chen, X., Xu, K., Wang, H.: 3d-aware object goal navigation via simultaneous exploration and identification. In: Proceedings of the IEEE/CVF Conference on Computer Vision and Pattern Recognition. pp. 6672–6682 (2023)
47. Zhao, Y., Xu, K., Zhu, Z., Hu, Y., Zheng, Z., Chen, Y., Ji, Y., Gao, C., Li, Y., Huang, J.: Cityeqa: A hierarchical llm agent on embodied question answering benchmark in city space. arXiv preprint arXiv:2502.12532 (2025), <https://arxiv.org/abs/2502.12532>
48. Zheng, D., Huang, S., Zhao, L., Zhong, Y., Wang, L.: Towards learning a generalist model for embodied navigation. In: Proceedings of the IEEE/CVF Conference on Computer Vision and Pattern Recognition (CVPR) (2024), https://openaccess.thecvf.com/content/CVPR2024/papers/Zheng_Towards_Learning_a_Generalist_Model_for_Embodied_Navigation_CVPR_2024_paper.pdf
49. Zhou, G., Hong, Y., Wu, Q.: Navgpt: Explicit reasoning in vision-and-language navigation with large language models. In: Proceedings of the AAAI Conference on Artificial Intelligence. vol. 38, pp. 7641–7649 (2024)
50. Zitkovich, B., Brohan, A., Brown, N., Carbajal, J., Chebotar, Y., Chen, X., et al.: Rt-2: Vision-language-action models transfer web knowledge to robotic control. In: Conference on Robot Learning (CoRL) (2023), <https://proceedings.mlr.press/v229/zitkovich23a.html>, pMLR